Open Archive TOULOUSE Archive Ouverte (OATAO)
OATAO is an open access repository that collects the work of Toulouse researchers and makes it freely available over the web where possible.

This is an author-deposited version published in : http://oatao.univ-toulouse.fr/
Eprints ID : 9166

To link to this article : DOI:10.1021/la3046548
URL : http://dx.doi.org/10.1021/la3046548

To cite this version : Pascaud, Patricia and Gras, Pierre and Coppel, Yannick and Rey, Christian and Sarda, Stéphanie. *Interaction between a bisphosphonate, tiludronate, and biomimetic nanocrystalline apatites.* (2013) Langmuir, vol. 29 (n° 7). pp. 2224-2232. ISSN 0743-7463

Any correspondance concerning this service should be sent to the repository administrator: staff-oatao@listes-diff.inp-toulouse.fr

Interaction between a Bisphosphonate, Tiludronate, and Biomimetic Nanocrystalline Apatites

Patricia Pascaud,[†] Pierre Gras,[‡] Yannick Coppel,[§] Christian Rey,[‡] and Stéphanie Sarda*[,†]

[†]CIRIMAT, INPT-CNRS-UPS, Université de Toulouse, Université Paul Sabatier, Toulouse, France

[‡]CIRIMAT, INPT-CNRS-UPS, Université de Toulouse, ENSIACET, Toulouse, France

[§]CNRS, LCC, Toulouse, France

Supporting Information

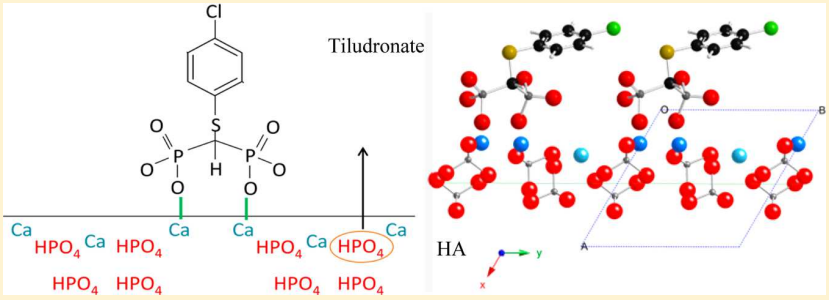

ABSTRACT: Bisphosphonates (BPs) are well established as successful antiresorptive agents for the prevention and treatment of bone diseases such as osteoporosis and Paget's disease. The aim of this work was to clarify the reaction mechanisms between a BP molecule, tiludronate, and the nanocrystalline apatite surface. The adsorption of tiludronate on well-characterized synthetic biomimetic nanocrystalline apatites with homogeneous but different compositions and surface characteristics was investigated to determine the effect of the nanocrystalline apatite substrate on the adsorption behavior. The results show that the adsorption of tiludronate on nanocrystalline biomimetic apatite surfaces varies over a large range. The most immature apatitic samples exhibited the highest affinity and the greatest amount adsorbed at saturation. Maturation of the nanocrystals induces a decrease of these values. The amount of phosphate ion released per adsorbed BP molecule varied, depending on the nanocrystalline substrate considered. The adsorption mechanism, although associated with a release of phosphate ions, cannot be considered as a simple ion exchange process involving one or two phosphate ions on the surface. A two-step process is proposed consisting of a surface binding of BP groups to calcium ions associated with a proton release inducing the protonation of surface orthophosphate ions and their eventual solubilization.

INTRODUCTION

Bisphosphonates (BPs) are well established as successful antiresorptive agents for the prevention and treatment of bone diseases such as osteoporosis and Paget's disease.[1] BPs were first studied over 30 years ago as synthetic analogues of inorganic pyrophosphate, characterized by a nonhydrolyzable P−C−P structure with two phosphonic acid groups bound to the same carbon. Their activity is related to both physicochemical and biological effects: like pyrophosphate, BPs present high affinities for adsorption onto apatite crystals and preventing mineral dissolution, and they have also been shown to inhibit osteoclasts activity.[2]

Several reports have been presented on the interaction of BPs with apatites, usually involving hydroxyapatite considered as a model of bone mineral,[3] but only a very few studies have been made on bone mineral itself or nanocrystalline apatites.[4,5] Associations of BPs with several calcium phosphate compounds have also been studied for the development of new strategies for local administration of BPs within osteoporotic sites exhibiting a risk of fracture (vertebra, hip, wrist, etc.) in order to limit a systemic application of the drug that may induce adverse effects.[6,7]

Although stoichiometric hydroxyapatite ($Ca_{10}(PO_4)_6(OH)_2$, HA), has often been used to study the adsorption properties of BPs, it appears rather different from bone mineral described as a nonstoichiometric nanocrystalline apatite (NCA) containing both carbonate and hydrogen-phosphate ions. One of the most interesting characteristics of bone mineral, evidenced by spectroscopic methods, is the existence of a structured hydrated surface layer that contains mineral ions in "non-apatitic" environments[8,9] and may affect its surface properties. During aging, the nanocrystalline apatite of bone, which is originally rich in surface nonapatitic environments and HPO_4^{2-} ions and poor in carbonate in embryonic bones, evolves toward a more stable carbonated apatite poorer in HPO_4^{2-} ions associated with a hydrated surface layer decrease.[10] Although natural bone

has also been used to study BPs adsorption, it appears as a heterogeneous mixture of apatite nanocrystals with different ages and compositions. If absorption studies on real bone are necessary, it might not be considered an ideal sample for analyzing the adsorption process mechanism.

In this study we planned to investigate the adsorption of a BP, tiludronate (Figure 1), on well-characterized synthetic

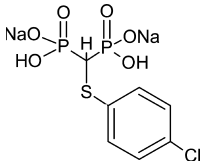

Figure 1. Chemical structure of tiludronate disodium salt.

nanocrystalline apatites with homogeneous but different compositions and surface characteristics, to determine the effect of the nanocrystalline apatite substrate on the adsorption behavior. Another aim of this work was also to clarify the reaction mechanisms between the BP molecule of this study, tiludronate (Figure 1), and the nanocrystalline apatite surface. Although several studies have reported the release of phosphate ions during the adsorption of several molecules, including BPs, suggesting an ion exchange reaction, this phenomenon has rarely been quantified, and the adsorption process remains unclear. Three synthetic nanocrystalline apatites were used with a wide variety of compositions and surface characteristics: an apatite rich in HPO_4^{2-} and exhibiting a well-developed hydrated surface layer, NCA1, which can be compared to freshly formed bone mineral; and two apatites aged in solution for 1 month, with a reduced hydrated surface layer, one obtained in the presence of carbonate and containing both carbonate and HPO_4^{2-} ions, NCA2, similar to mature bone mineral, and another one obtained in the absence of carbonate and containing only HPO_4^{2-} ions, NCA3. The interaction phenomena between tiludronate molecules and these apatite nanocrystals were determined through adsorption reactions involving physicochemical characterization of the solid and the liquid. These data give new insight into the role of nanocrystalline apatites characteristics in bone reactivity and possible drug delivery applications.

EXPERIMENTAL SECTION

Materials. Nanocrystalline apatite powders were synthesized by a double decomposition technique at ambient temperature and physiological pH. NCA1 was prepared by pouring a calcium nitrate solution ($Ca(NO_3)_2{,}4H_2O$, C = 69.6 g/L, 750 mL) into an ammonium phosphate solution with an excess of phosphate ions for buffering the solution ($(NH_4)_2HPO_4$, C = 80g/L, 1500 mL). The precipitate obtained was quickly vacuum filtered, washed with deionized water, and freeze-dried. Then the powder was sieved (<125 μm) and stored in a freezer. NCA2 was prepared using the same experimental conditions by pouring a calcium solution into a sodium carbonate and ammonium phosphate solution ($(NH_4)_2HPO_4$, C = 80g/L, $NaHCO_3$, C = 60g/L, 1500 mL), and the precipitate obtained was left to mature 1 month at room temperature before filtration, washing and freeze-drying. NCA3 is an apatite rich in OH^- and poor in HPO_4^{2-} ions and with very few carbonate ions. It was introduced in the study to evaluate the effect of carbonate species on the adsorption properties and can be compared to early dental enamel. It was prepared similarly to NCA2, by pouring a calcium solution into a phosphate solution, without adding carbonate. The precipitate obtained was left to mature 1 month and then filtered, washed, and freeze-dried.

Powdered tiludronate (disodium((4-chlorophenyl)thio)methylene-bis-phosphonate) hemihydrate was a gift from Sanofi Aventis (France).

Adsorption Experiments. The adsorption experiments were carried out by dispersing 50 mg of poorly crystalline apatite powders in 5 mL of adsorption medium, an aqueous solution of tiludronate (1 mM KCl) adjusted to physiological pH by addition of KOH and HCl solutions. The suspensions were sonicated for a few minutes and incubated for 2 h at physiological temperature without stirring. After centrifugation at 5000 rpm for 20 min, the supernatants obtained were filtered onto Millipore filters (pore size 0.2 μm) before chemical analyses. The powders were washed with deionized water, freeze-dried ,and stored in a freezer.

Characterization Techniques. The phosphate content of each synthesized nanocrystalline apatite was determined by spectrometry of the phosphovanadomolybdic acid complex and the calcium content by complexometry.[11] The level of carbonate ions in the apatite compounds was evaluated by coulometric techniques (UIC, Inc. CM 5014 coulometer with CM 5130 acidification unit). The specific surface area of each sample was measured by the Brunauer–Emmett–Teller (BET) method using a Quantachrome Instruments Monosorb Nova 1000.

The solutions were analyzed for tiludronate and mineral ions content. The tiludronate concentration in solution was determined by means of UV adsorption spectroscopy at 265 nm (Single beam UV/vis Hitachi U-1100 spectrophotometer), and the phosphate ion concentration was determined by colorimetry at 460 nm. The amount of calcium was obtained by inductively coupled plasma atomic emission spectroscopy (Horiba, Jobin Yvon, 2004, Ultima 2, ICP-AES).

The solid phases before and after adsorption of tiludronate were characterized by X-ray diffraction (XRD) (Seifert XRD-3000TT diffractometer, CuKα1 radiation with λ = 1.5406 Å) and the apparent crystallite sizes were calculated from the (310) and (002) lines, applying Scherrer's formula.[12] They were analyzed by different spectroscopic techniques. Fourier transform infrared (FTIR) analysis was performed using a Thermo Nicolet 5700 FTIR spectrometer (2 mg sample/300 mg KBr), covering the 4000–400 cm^{-1} range at 64 scans accumulation and 4 cm^{-1} resolution. NMR solid-state experiments were recorded on a Bruker Avance 400 (9.4 T) spectrometer equipped with a 4 mm probe. Samples were spun at 8 kHz at the magic angle using ZrO_2 rotors. For ^{31}P magic angle spinning (MAS) single-pulse experiments, small flip angles (~30°) were used with recycle delays of 20 s and with high-power proton decoupling conditions. For $^1H \rightarrow ^{31}P$, the cross-polarization (CP) MAS recycle angle used was 5 s with contact times τ = 0.1 ms. ^1H and ^{31}P chemical shifts were referenced to external tetramethylsilane (TMS) and 85% H_3PO_4 samples, respectively. Transmission electron microscopy (TEM) micrographs were recorded in the secondary electron mode on a JEOL JEM 2100F microscope set at an acceleration tension of 200 kV.

RESULTS

Characterization of the Biomimetic Nanocrystalline Apatites. Considering the complexity of biomimetic apatite nanocrystals, a careful characterization of the adsorption substrates was performed. The solids obtained exhibited XRD patterns (Figure SI1, Supporting Information) characteristic of poorly crystalline apatites.[10] NCA3 obtained in the absence of carbonate salt appeared to be better crystallized than NCA1 and NCA2. The apparent crystallite sizes, calculated from the (310) and (002) lines, are reported in Table 1. The crystals exhibited an elongated shape along the c axis direction. Nanocrystal length was smaller for the powders obtained without maturation and without carbonate (NCA1). NCA3 crystals obtained in the absence of carbonate appeared longer than NCA2 in agreement with other reports on the effect of

Table 1. Apparent Crystallite Sizes Calculated from the (310) and (002) XRD Lines for NCA1, NCA2, and NCA3

sample	$L(310) \pm 3$ Å	$L(002) \pm 3$ Å
NCA1	28	148
NCA2	43	167
NCA3	41	209

carbonate ions on apatites crystallinity and crystal growth inhibition.[13,14]

TEM observations of NCA1 and NCA2 showed small elongated plates less than 10 nm thick (Figure 2), analogous to

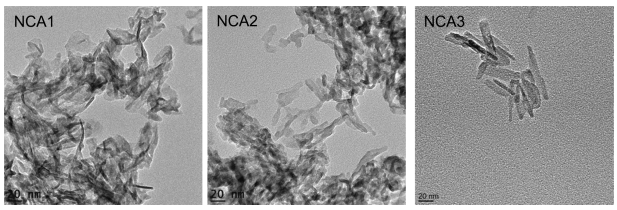

Figure 2. TEM observations of the nanocrystalline apatites NCA1, NCA2, and NCA3.

those found for bone mineral.[15] For NCA3, the crystals looked needle-shaped with little difference between width and thickness, as it is usually the case for enamel apatites and more generally for synthetic hydroxyapatite.

The specific surface area was the largest for the apatite freshly precipitated without maturation, NCA1 (Table 2). In the presence of carbonate, in NCA2, maturation did not present a significant effect on the specific surface area, in agreement with XRD and TEM results. Similar observations have already been reported.[8] In the absence of carbonate, however, crystal growth occurs during maturation (NCA3).

FTIR spectra of the apatitic powders synthesized (Figure 3A) showed the characteristic vibration bands of poorly crystalline apatites: especially apatitic PO_4^{3-} vibration bands at 469 ($\nu 2$), 562–603 ($\nu 4$), 962 ($\nu 1$), and 1000–1104 cm^{-1} ($\nu 3$).[10] NCA2 presents bands at 870, 1420, and 1470 cm^{-1}, due to CO_3 vibrations characteristic of nonapatitic carbonates and type B carbonate species. The decomposition of the ν_4 PO_4 domains allows the detection of a set of lines that have been assigned to apatitic HPO_4^{2-} (550 cm^{-1}) and the presence of nonapatitic environments of PO_4^{3-} (617 and 634 cm^{-1}) and HPO_4^{2-} ions (533 cm^{-1}) present in the surface hydrated layer.[8] Curve-fitting analysis of the FTIR spectra of nanocrystalline apatites in the ν_4PO_4 domain using GRAMS/386 software (Figure 4A) allows a quantitative evaluation of the integrated intensities of the lines assigned to these species (Figure 4B),.[8,16] As expected, NCA1 contains a large amount of labile HPO_4^{2-} in the surface hydrated layer, which decreases considerably in the matured samples. In addition, NCA3, matured in the absence of carbonate, clearly showed OH^- lines, which were barely detected in other samples. These results are in agreement with previous studies, and the synthesized nanocrystals exhibit different bulk and surface compositions as expected.[10]

The chemical composition of the synthesized samples is reported in Table 2. The Ca/P ratio appears very low for the apatite without maturation, NCA1. An increase in this ratio was observed with maturation time as previously published by several authors.[17,18] However, this increase in the Ca/P ratio has different origins. In the highly carbonated apatite, NCA2, phosphate ions were substituted by carbonate ions in the apatite domains and in the surface layer, and the increased Ca/P ratio was essentially due to this substitution, resulting in a decrease in phosphate content. The Ca/(P+C) ratio, which is more representative of the composition of these apatites, does not appear to be much different from that of NCA1, indicating that HPO_4^{2-} ions were replaced by CO_3^{2-} during the maturation process, which did not alter the calcium content of the apatite. This is not the case with NCA3, which exhibits a higher Ca/(P+C) ratio than the other samples. In this case, the increase in the Ca/P ratio can be assigned to an evolution toward an hydroxyapatite closer to stoichiometry.

The ^{31}P NMR spectra of NCA1, NCA2, and NCA3 (Figure 5A) all present a broad signal with asymmetric pattern at about 3 ppm attributable in apatite samples to orthophosphate species.[19] This asymmetric signal is reported in the literature for bone mineral between 2–3 ppm[4,20,21] and for stoichiometric HA at 2.8 and 3.1 ppm.[9,22] For all samples, the comparison of ^{31}P MAS and ^1H–^{31}P CP MAS NMR spectra evidence the presence of at least two different types of signal: a sharp one due to crystalline apatite, and a broader one. The intensity of the broad signal strongly increased with short CP contact time (100 μs), and it can be associated with the presence of HPO_4^{2-} ions in these samples, like in bone[9] or similar nanocrystalline apatites.[23,24] These HPO_4^{2-} ions have been shown to belong to the hydrated layer at the surface of the nanocrystals. From the ^{31}P MAS spectra, the quantity of HPO_4^{2-} ions appears to be more important for NCA1 compared with NCA2 and NCA3, which shows the lowest amount. Furthermore, the signals are broader for NCA1 compared to NCA2 and NCA3, indicating a higher structural disorder for NCA1. These results confirm that the asymmetry is due to the presence of HPO_4^{2-} species, as previously published.[25] NCA3 shows a rather low line breadth evidencing the influence of the maturation on the crystallinity, as NMR line width decrease has been shown to be due to an increase in crystallinity.[23] However, this phenomenon was not observed for NCA2 due to the effect of internal strains associated with the presence of carbonate ions.[14]

Adsorption of Tiludronate. Preliminary kinetic tests showed that the adsorption equilibrium involving tiludronate was reached rather rapidly after about 20 min (Figure SI2), as observed for other BPs.[26]

The evolution of the amount of tiludronate adsorbed Qads (μmol/m^2) on the nanocrystalline apatites from dilute aqueous solutions (0–4 mM) as a function of the equilibrium concentration in solution Ceq (mmol/L) are plotted in Figure

Table 2. Chemical Analysis and Specific Surface of NCA1, NCA2, and NCA3

sample	Ca (wt %)	P (wt %)	CO_3 (wt %)	Ca/P	Ca/(P+C)	specific surface (m^2/g)
NCA1	32.59 ± 0.29	17.96 ± 0.31	0.34 ± 0.04	1.40 ± 0.02	1.39 ± 0.02	193.26 ± 2.78
NCA2	34.43 ± 0.74	16.51 ± 0.22	5.57 ± 0.40	1.62 ± 0.02	1.38 ± 0.02	189.87 ± 4.52
NCA3	36.82 ± 0.42	17.72 ± 0.45	0.54 ± 0.04	1.61 ± 0.02	1.59 ± 0.02	153.67 ± 4.94

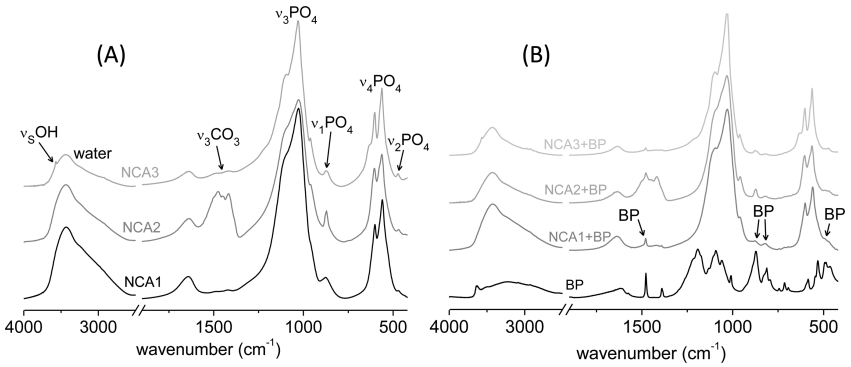

Figure 3. FTIR spectra of nanocrystalline apatites (A) before adsorption of tiludronate (NCA1, NCA2, NCA3), (B) after adsorption (NCA1+BP, NCA2+BP, NCA3+BP) and tiludronate (BP).

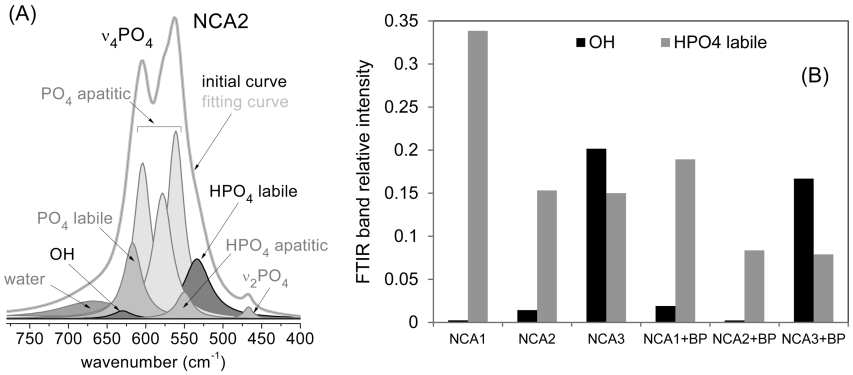

Figure 4. (A) Decomposition of FTIR spectra of NCA2. (B) Relative intensity of FTIR labile HPO_4 and hydroxyl bands in the ν_4 PO_4 domain of nanocrystalline apatites before adsorption (NCA1, NCA2, NCA3) and after adsorption of tiludronate (NCA1+BP, NCA2+BP, NCA3+BP).

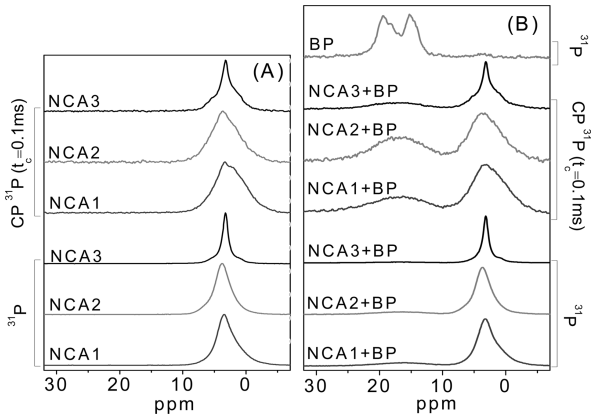

Figure 5. ^{31}P MAS and ^{1}H−^{31}P CP MAS NMR solid state spectra, (A) nanocrystalline apatites before adsorption (NCA1, NCA2, NCA3) and (B) after adsorption of tiludronate (BP, NCA1+BP, NCA2+BP, NCA3+BP).

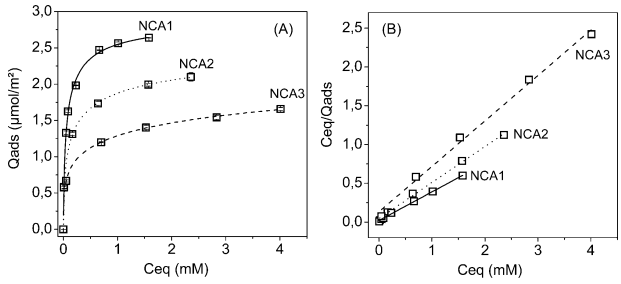

Figure 6. (A) Adsorption isotherms and (B) Langmuir linear regressions of Langmuir adsorption isotherms of tiludronate by NCA1, NCA2, NCA3 from dilute aqueous solutions using Langmuir linear equation plotting Ceq/Qads versus Ceq.

6A. The adsorption plateau was reached at rather low concentration, indicating the high affinity of tiludronate for the surfaces of the nanocrystals. The plateau value appears at a higher Qads value for the NCA1 sample than for NCA2 and NCA3.

Several equations were used to fit the data: Langmuir, Langmuir−Töth, and Langmuir−Freundlich. The adsorption isotherms of all the nanocrystalline apatites synthesized fit best with a Langmuir type isotherm (for example, with the NCA1 sample, R^2 = 0.999, 0.996, and 0.944, respectively) as has usually been found in other studies.[26] According to the Langmuir isotherm,

$$Q_{ads} = N \times \frac{(K \times C_{eq})}{1 + (K \times C_{eq})} \quad (1)$$

we can calculate the parameters of adsorption (Table 3), i.e., the affinity constant of tiludronate for the nanocrystals surface (K (L/mmol)) and the amount adsorbed at saturation (N (μmol/m^2)), (Figure 6B).

$$\frac{C_{eq}}{Q_{ads}} = \frac{C_{eq}}{N} + \frac{1}{(K \times N)} \quad (2)$$

Table 3. Parameters of Adsorption from the Langmuir Equation and the Ion Exchange Equation for NCA1, NCA2, and NCA3

	Langmuir		ionic exchange	
sample	N (μmol/m^2)/ N (*mmol/g*)	K (L/mmol)	N (μmol/m^2) /N (*mmol/g*)	Ke
NCA1	2.710 ± 0.006/ *0.53 ± 0.01*	18.48 ± 0.86	2.90 ± 0.05/ *0.56 ± 0.01*	42.4 ± 0.1
NCA2	2.17 ± 0.02/ *0.41 ± 0.01*	10.13 ± 1.27	2.42 ± 0.06/ *0.46 ± 0.01*	15.6 ± 0.1
NCA3	1.69 ± 0.03/ *0.26 ± 0.01*	4.44 ± 0.97	2.05 ± 0.07/ *0.32 ± 0.01*	7.15 ± 0.12

Moreover, we can evaluate the surface area δ (m^2) occupied by one molecule of tiludronate adsorbed at saturation on the surface of a nanocrystal (with Na: Avogadro's number):

$$\delta = \frac{1}{N \times \mathrm{Na}} \tag{3}$$

The adsorption parameters are shown in Table 3. The values obtained are similar to those generally reported for BP adsorption.[26] The surface area δ (nm^2) calculated occupied by one molecule of tiludronate adsorbed at saturation on the surface of the nanocrystals varied from 0.61 (NCA1) to 0.77 (NCA2) and 0.98 (NCA3). According to these data, the adsorption capacity at saturation varies strongly with the type of apatite nanocrystals and allows a classification: NCA1 > NCA2 > NCA3. Similar observations have already been noted previously for the adsorption of risedronate on several apatitic calcium phosphates using similar experimental conditions.[27] These studies showed that higher amounts of BPs adsorbed at saturation were obtained on NCA compared to well-crystallized stoichiometric HA, and this behavior was related to the presence of a hydrated surface. Moreover, some authors have shown that the affinity constant varies strongly depending on the nature of the adsorbing BP molecules.[3] It is also the case in this study.

Mineral Ions Composition of the Solution after Adsorption. During adsorption of BPs on apatites, release of phosphate ions has often been reported; however, quantitative data are scarce. The evolution of the mineral content of the solution is shown in Figure 7. No significant evolution in the pH value of the solution was observed during the adsorption experiments. The point related to Qads equal to zero corresponds to a blank assay performed under the same conditions as the adsorption experiments but without tiludronate.

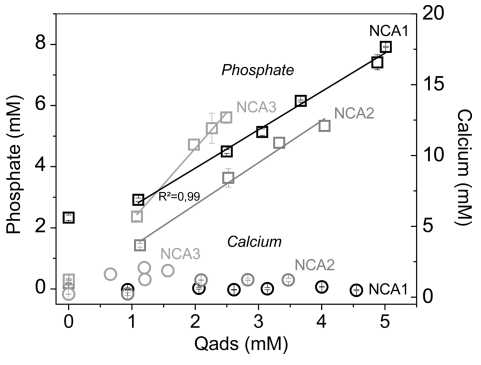

Figure 7. Concentration of phosphate and calcium ions in the supernatants upon adsorption of tiludronate on NCA1, NCA2, and NCA3.

The content of calcium ions in solution remains very low (less than 3 ppm) and does not seem related to the amount of tiludronate adsorbed. The calcium in solution can be related to the dissolution of the nanocrystals in aqueous solution. However, if a dissolution equilibrium with the apatite phase was reached, the calcium concentration should decrease when the phosphate content increases in solution, which is not the case.

For the blanks (without tiludronate), the corresponding amount of phosphate ions in solution appears to be much higher for the nonmaturated and noncarbonated support NCA1 (2.47 ± 0.18 ppm) than for the maturated ones: carbonated NCA2 (0.30 ± 0.03 ppm) and noncarbonated NCA3 (0.25 ± 0.06 ppm). These results can be related to the dissolution of the apatites and the reported metastable solubility equilibrium reached with these compounds, as reported in the case of bone mineral.[14] The Ca/P atomic ratio in solution in the blanks can be evaluated as 0.63, 1.53, and 0.68 for NCA1, NCA2, and NCA3, respectively. The Ca/P ratio in solution is different from that in the powders, and characteristic of a noncongruent dissolution. This phenomenon appears weaker for NCA2, probably because carbonate anions are also dissolved, thus increasing the content of the counterion, Ca^{2+}, in solution. This noncongruent dissolution has already been observed in other studies and been associated with the maturation process of nanocrystalline apatites and, probably, calcium surface adsorption.[8,28]

For the supports with tiludronate, the concentration of phosphate ions in solution increased linearly with the amount of tiludronate adsorbed. The slope of the straights line, however, is different depending on the nanocrystalline apatite: it is equal to 1.26 ± 0.05 for NCA1, 1.37 ± 0.12 for NCA2, and 2.35 ± 0.16 for NCA3. Therefore, the number of phosphate groups released per single adsorbed molecule of tiludronate (corresponding to the slope) varies depending on the nanocrystalline apatite considered.

Powder Characterization after Adsorption. The solids obtained after adsorption of tiludronate were analyzed by XRD (Figure SI1). All the samples exhibited XRD patterns characteristic of poorly crystalline apatites. The presence of tiludronate did not have any influence on the crystallinity, and no additional crystalline solid phase was observed after adsorption. According to TEM observations of the nanocrystals after adsorption (data not shown), the adsorption of tiludronate did not alter the morphology of the nanocrystals, and no other particles with different morphologies were detected.

FTIR spectra of the original tiludronate molecule and of the nanocrystalline apatites after adorption are shown in Figure 3B.[29] The spectrum of tiludronate presents several lines, particularly those associated with C–C aromatic vibrations at 1480, 1500, 1580, and 1620 cm^{-1}, and others attributable to C–H vibration at 1390 and 820 cm^{-1} and C–S vibrations at 710 cm^{-1}. After adsorption, the spectra of all the NCA displayed additional bands and shoulders characteristic of tiludronate molecules, especially at 1480 cm^{-1} and 820 cm^{-1}. The other vibration bands of tiludronate molecules, especially those of the phosphonate groups, were hidden by those of phosphate groups on the nanocrystalline apatitic supports. Curve-fitting analysis of FTIR spectra of nanocrystalline apatites after adsorption using GRAMS/386 software presented

some difficulties due to the presence of tiludronate vibration bands in the ν_4 PO_4 domain. Such analyses must take into account the contributions of tiludronate vibration bands at 715, 690, and 490 cm^{-1} (C–S and C–H domains), (Figure 3B). Nevertheless, the results of curve-fitting analysis of the powders after adsorption (Figure 4B) show a decrease in labile HPO_4^{2-} environments for the NCA1 and NCA2 compounds, partially attributable to the maturation process of the powders during the adsorption experiment and partly to the adsorption of tiludronate, in accordance with an ion exchange process.

The ^{31}P NMR spectra of tiludronate and nanocrystalline apatites after adsorption are shown in Figure 5B. The spectrum of tiludronate shows two distinct lines at about 15.2 ppm and 19.4 ppm attributable to the ^{31}P nuclei of the two phosphonate groups, which are chemically nonequivalent in the sodium tiludronate. The spectra of the nanocrystals after adsorption showed a broad asymmetric signal at about 3 ppm due to orthophosphates and HPO_4 species. In addition, all spectra presented a weaker broad line at 17 ppm at about the chemical shift of phosphonate groups of tiludronate. A similar broad line has already been observed in previous studies concerning the adsorption of some BPs on bone and hydroxyapatite.[4,20,22] Grossmann et al. suggested that the broadness of this line is due to structural heterogeneities of the BP structure after adsorption. $^1H \rightarrow ^{31}P$ CP MAS RMN spectra of the nanocrystals after adsorption are presented in Figure 5B. In all spectra, the broad line attributed to tiludronate appears stronger, and the dissymmetry of the main orthophosphate line is increased compared with the single pulse spectra. Moreover, the line corresponding to the adsorbed tiludronate was enhanced in the cross-polarized spectra but remained very broad and featureless, confirming the alteration in the phosphonate environments of tiludronate after adsorption compared to the sodium salt.

DISCUSSION

The data obtained clarify the mechanism of BPs adsorption and, more specifically, the relationship between BPs adsorption on nanocrystalline apatite and phosphate ion release. In addition, the adsorption characteristics were found to strongly depend on the composition and nature of the nanocrystals.

Mechanism of Tiludronate Adsorption. The phosphate ion release in solution can have several origins and does not necessarily correspond to an adsorption reaction. The other possible phenomenon also reported in a few cases with BPs[30] is a chemical displacement reaction involving the formation of a calcium BP (tiludronate) salt and the dissolution of the calcium phosphate. This phenomenon could occur, especially with the most soluble apatite, NCA1, and has already been reported in the case of zoledronate adsorption on β-TCP.[5] Such a reaction could be written as follows:

$$Ca_X(PO_4)_{solid} + (X/2)BP^{4-}{}_{solution} \rightarrow X/2Ca_2BP_{solid} + (PO_4)^{2X-}{}_{solution} \quad (4)$$

where X is the Ca/P ratio of the apatite, and (PO_4) represents phosphate species with undetermined protonation states. In this case, the $P_{released}$/BP ratio would be 2/X for the formation of the Ca_2BP salt and 1.43, 1.23, and 1.24 for NCA1, NCA2, and NCA3, respectively. For the formation of the CaBP salt, the $P_{released}$/BP ratio would be 1/X, that is, 0.71, 0.61, and 0.61 for NCA1, NCA2, and NCA3 respectively. These last values do not obviously fit with the experimental ones, and the formation of CaBP salt can be discarded; however, the expected values for the formation of Ca_2BP are closer, especially for NCA2, and a doubt could exist, but they appear significantly different for NCA1 and NCA3. Other arguments excluding the precipitation of a calcium salt of BP and the dissolution of the apatite are:

- the absence of formation of other crystalline phases according to XRD, although the formation of an amorphous calcium-BP salt could be possible;
- TEM micrografts showing similar crystals before and after adsorption and the absence of amorphous component;
- the observation of a Langmuir type isotherm with a plateau is also characteristic of an adsorption process: the continuous addition of BP should lead, in case of a dissolution-reprecipitation process, to a continuous uptake of BP without a plateau;
- the coherent values of the surface occupied by one adsorbed tiludronate molecule.

There are, however, other reactions susceptible to releasing phosphate ions: dissolution of the nanocrystals, the maturation process of the nanocrystalline apatites during the time of adsorption, and BP uptake releasing surface phosphate groups. The dissolution and maturation effects can be observed for the blanks (apatite powders dispersed in adsorption medium without tiludronate, corresponding to Qads = 0). For NCA2 and NCA3, the concentrations of phosphate in solution for blank experiments are rather low, and it can be assumed that the increase of phosphate concentration is related to the adsorption. For NCA1, the phosphate concentration is much higher in the blank; however, it seems unlikely that the increase in phosphate concentration observed during the adsorption of tiludronate would correspond to an increase of dissolution and/or maturation rate. Thus, in all cases, the release of phosphate with the amount of tiludronate adsorbed seems to correspond mainly to a substitution reaction with surface phosphate groups, as hypothesized by several authors.[26] Indeed, a linear correlation exists between the concentration of phosphate ions released in solution and the number of tiludronate molecules adsorbed. Although several reports mentioned a release of phosphate ions related to the adsorption of BPs or other molecules, only a few exchange ratios have been determined. For the adsorption of risedronate on the surface of stoichiometric hydroxyapatite, Errassifi et al. reported an ion exchange between one molecules of BP in solution and one phosphate ion on the apatitic surface. Mukherjee et al. suggested two exchange processes involving either one or two phosphate ions displaced for one BP molecule, depending on the nature of the BPs molecules. However, in this study, the exchange ratio is not equal to one or two and appears to be different for the nanocrystalline apatites considered. Such an exchange reaction could be written:

$$\alpha Phos_{apatite} + BP_{solution} \Leftrightarrow BP_{apatite} + \alpha Phos_{solution} \quad (5)$$

In this chemical equation, Phos represents an undetermined phosphate species, at this stage in our studies, corresponding to a surface orthophosphate group, PO_4^{3-}, HPO_4^{2-}, or possibly a mixture. Similarly, the protonation state of the tiludronate molecules involved could not be determined. This reaction can be treated as an exchange equilibrium:

$$\mathrm{Ke} = \frac{[\mathrm{BP}_{\mathrm{apatite}}] \times [\mathrm{Phos}_{\mathrm{solution}}]^{\alpha}}{[\mathrm{Phos}_{\mathrm{apatite}}]^{\alpha} \times [\mathrm{BP}_{\mathrm{solution}}]} = \frac{Q_{\mathrm{ads}} \times \mathrm{Phos}_{\mathrm{solution}}{}^{\alpha}}{[\alpha(N - Q_{\mathrm{ads}})]^{\alpha} \times C_{\mathrm{eq}}} \quad (6)$$

that can be linearized as

$$\frac{Q_{\mathrm{ads}}{}^{1/\alpha} \times \mathrm{Phos}_{\mathrm{sol}}}{C_{\mathrm{eq}}{}^{1/\alpha}} = K_{\mathrm{e}}{}^{1/\alpha} \times N - K_{\mathrm{e}}{}^{1/\alpha} \times \alpha \times Q_{\mathrm{ads}} = f(Q_{\mathrm{ads}}) \quad (7)$$

This equation allows the calculation of new, more realistic parameters considering the complete reaction: the exchange constant Ke and the adsorption at saturation *N*. These values were determined in the case of tiludronate using the total phosphate concentration in solution, as the speciation of the phosphate groups involved in the exchange is unknown (Table 3). The ion exchange constant, Ke, appears to be very different for the three nanocrystalline apatites, which can be ranked in the following order: NCA1 > NCA2 > NCA3. The same order is observed for the saturation limit *N*.

The description of the adsorption reaction of BPs as an ion exchange reaction clarifies the behavior of the BP–apatite association and especially the nonreversibility of the reaction upon dilution. Once attached, the BP–apatite compounds cannot be washed out. It is only in the presence of phosphate ions in the solution that a reverse reaction is possible.[26] Several questions remain unanswered, however, such as the substitution process and the reason for a variable phosphate release.

Molecular Model for Tiludronate on NCA. Mukherjee et al.[4] have proposed two processes for BP adsorption: one involving the removal of one phosphate ion from the surface, and another involving the removal of two phosphate ions. According to these authors, the adsorption process is determined by the type of BP involved and specifically by the free adsorption energy. In our case, tiludronate would be classified among BPs that remove only one phosphate group from the surface according to their classification. Our results indicate, however, that the phosphate release also varies according to the type of nanocrystalline apatite considered and does not depend only on the type of BP molecule. An interesting model has been provided by this group[4]showing the substitution of one phosphate group by one BPs molecule (pamidronate) on the (001) crystallographic plane of the apatite.

In the case of nanocrystalline apatites, however, the largest crystal surface corresponds more likely to a (100)-type plane parallel to the *c* axis of the hexagonal structure. In addition, the hydrated surface layer disturbs the atomic arrangement compared to a well-crystallized stoichiometric apatite.

The substitution of two phosphates seems more difficult and raises questions. The average distance between two P atoms in a BP molecule is close to 3.3 Å, and it seems difficult to substitute two close phosphate groups in the apatite structure; the distance between is at least 4.1 Å. In a single (100) face, the distance between phosphate groups is even larger (6.9 Å). This substitution mechanism thus seems unrealistic. If a surface hydrated model like that of octacalcium phosphate (OCP) is considered as a model of nanocrystals hydrated surface,[31] the same difficulties, can be raised and the minimum distance between two orthophosphate groups appears to be close to that found for HA. In addition, the observation of noninteger values of the exchange ratio would lead one to consider a variable amount of phosphate ions displaced even above 2 in one case.

Other binding mechanisms of BP on apatites have been proposed involving, not a phosphate substitution, but an interaction with calcium groups of the surface.[32] In this case, the atomic distances are coherent, and such an interaction appears possible even with two calcium ions on the surface.

Considering the variable number of phosphate ions released per BP molecule adsorbed, and the impossibility of substituting two orthophosphate groups, one may then suggest an adsorption process in two steps: (1) an interaction of a BPs molecule with calcium ions on the surface leading to partial or total deprotonation of the phosphonate groups; (2) the released protons interact with surface hydrogenphosphate groups, yielding $H_2PO_4^-$ ions, which are then released. It seems probable that these reactions strongly alter the structure of the surface layer.

In this schema, the released phosphate groups may vary depending on the BPs molecules and the substrate, being more specifically related to the deprotonation of the BP molecules and the corresponding acidity constant of the bisphosphonic acids, the binding ability of these species to the surface calcium ions, the composition of the hydrated layer, and the relative content of orthophosphate (and carbonate) species. It should also be noted that several types of binding of BP molecules to calcium ions on the surface can be proposed: bidentate binding to one calcium ion or monodentate binding to two different calcium ions. At this stage, the data obtained do not allow these two possibilities to be discriminated. Additional investigations and adsorption modelizations could bring answers to these questions.

Thus the most mature sample, which exhibits the thinnest surface layer, releases the most phosphate ions per molecule adsorbed. The carbonated apatite releases less phosphate; however, carbonate ions could also be involved in the exchange process. The adsorption on freshly precipitated apatite, which presents the most developed hydrated layer, releases the fewest phosphate groups.

Although the adsorption reaction can be described as a two-step process, the global model of the ion exchange, with a noninteger number of phosphate ions, remains valid and complies with the data. This model explains the apparent irreversibility of the adsorption reaction on dilution, and the very limited release of BP in aqueous media. Additional work should be done to study the effect of soluble phosphate ions on the release of adsorbed BP molecules.

■ CONCLUSION

The adsorption of a BP, tiludronate, on nanocrystalline biomimetic apatite surfaces with different compositions and hydrated layer fractions varies over a large range. The most immature samples exhibited the highest affinity and the greatest amount adsorbed at saturation. Maturation of the nanocrystals induces a decrease of these values. The number of phosphate ions released per adsorbed BP molecule varied over a large range, depending not only on the type of BPs as shown by Mukherjee et al. but also on the nanocrystalline substrate considered. These data show that the adsorption mechanism, although associated with a release of phosphate ions, cannot be

considered as a simple ion exchange process involving one or two phosphate ions on the surface. A two-step process is proposed consisting of a surface binding of BP groups to calcium ions associated with a proton release inducing the protonation of surface orthophosphate ions and their eventual solubilization. This work shows that synthetic compounds can be used to explore the adsorption of drugs and more generally any chemical interaction related to the composition and surface properties of biological calcium phosphate nanocrystals without the burden of heterogeneity, variable behavior, and irreproducibility peculiar to calcium phosphates of biological origin.

■ ASSOCIATED CONTENT

Supporting Information

Figures SI1 and SI2. This material is available free of charge via the Internet at http://pubs.acs.org.

■ AUTHOR INFORMATION

Corresponding Author

*E-mail: stephanie.sarda@iut-tlse3.fr.

Notes

The authors declare no competing financial interest.

■ ACKNOWLEDGMENTS

The authors thank Sanofi Aventis for generously providing the tiludronate (disodium((4-chlorophenyl)thio)methylene-bisphosphonate) hemihydrate sample.

■ REFERENCES

(1) Russell, R. G. G.; Watts, N. B.; Ebetino, F. H; Rogers, M. J. Mechanisms of action of bisphosphonates: Similarities and differences and their potential influence on clinical efficacy. *Osteoporosis Int.* **2008**, *19* (6), 733−759.

(2) Rodan, G. A; Fleisch, H. A. Bisphosphonates: Mechanisms of action. *J. Clin. Invest.* **1996**, *97* (12), 2692.

(3) Nancollas, G. H.; Tang, R.; Phipps, R. J.; Henneman, Z.; Gulde, S.; Wu, W.; Mangood, A.; Russell, R. G; Ebetino, F. H. Novel insights into actions of bisphosphonates on bone: Differences in interactions with hydroxyapatite. *Bone* **2006**, *38* (5), 617−27.

(4) Mukherjee, S.; Song, Y.; Oldfield, E. NMR investigations of the static and dynamic structures of bisphosphonates on human bone: A molecular model. *J. Am. Chem. Soc.* **2008**, *130* (4), 1264−1273.

(5) Josse, S.; Faucheux, C.; Soueidan, A.; Grimandi, G.; Massiot, D.; Alonso, B.; Janvier, P.; Laïb, S.; Pilet, P.; Gauthier, O.; Daculsi, G.; Guicheux, J.; Bujoli, B.; Bouler, J.-M. Novel biomaterials for bisphosphonate delivery. *Biomaterials* **2005**, *26* (14), 2073−2080.

(6) Coleman, R. E. Risks and benefits of bisphosphonates. *Br. J. Cancer* **2008**, *98* (11), 1736−1740.

(7) Coleman, R.; Burkinshaw, R.; Winter, M.; Neville-Webbe, H.; Lester, J.; Woodward, E.; Brown, J. Zoledronic acid. *Expert Opin. Drug Saf.* **2011**, *10* (1), 133−145.

(8) Rey, C.; Combes, C.; Drouet, C.; Sfihi, H.; Barroug, A. Physico-chemical properties of nanocrystalline apatites: Implications for biominerals and biomaterials. *Mater. Sci. Eng., C* **2007**, *27* (2), 198−205.

(9) Wu, Y.; Ackerman, J. L.; Strawich, E. S.; Rey, C.; Kim, H. M; Glimcher, M. J. Phosphate ions in bone: Identification of a calcium−organic phosphate complex by 31P solid-state NMR spectroscopy at early stages of mineralization. *Calcif. Tissue Int.* **2003**, *72* (5), 610−26.

(10) Eichert, D.; Drouet, C.; Sfihi, H.; Rey, C.; Combes, C. Nanocrystalline apatite-based biomaterials: Synthesis, processing and characterization. *Biomater. Res. Adv.* **2008**, 93.

(11) Charlot, G. *Chimie Analytique Quantitative*; Masson et Cie: Paris, 1974.

(12) Guinier, A. *Théorie et Technique de la Radiocristallographie*, 3rd ed.; Dunod: Paris, 1964.

(13) LeGeros, R. Z.; Kijkowska, R.; Bautista, C.; LeGeros, J. P. Synergistic effects of magnesium and carbonate on properties of biological and synthetic apatites. *Connect. Tissue Res.* **1995**, *33* (1−3), 203−9.

(14) Baig, A. A.; Fox, J. L.; Hsu, J.; Wang, Z.; Otsuka, M.; Higuchi, W. I; LeGeros, R. Z. Effect of carbonate content and crystallinity on the metastable equilibrium solubility behavior of carbonated apatites. *J. Colloid Interface Sci.* **1996**, *179* (2), 608−617.

(15) Kim, H. M.; Rey, C.; Glimcher, M. J. Isolation of calcium-phosphate crystals of bone by non-aqueous methods at low temperature. *J. Bone Miner. Res.* **1995**, *10* (10), 1589−1601.

(16) Combes, C.; Rey, C.; Mounic, S. Identification and evaluation of HPO_4 ions in biomimetic poorly crystalline apatite and bone mineral. *Key Eng. Mater.* **2000**, *192*, 143−146.

(17) Menbaoui, A.; Barroug, A.; Lebugle, A.; Rey, C.; Legrouri, A.; Bennani, M.; Taitai, A. Interaction de l'héparine avec des phosphates de calcium biologiques. In *COVAPHOS 1: International Conference on the Valorization of Phosphate and Phosphorous Compound*, Marrakech, Marrocco, October 2004.

(18) Legros, R. Apport de la physico-chimie à l'étude de la phase minérale des tissus calcifiés. Masters Thesis, INP Toulouse, Toulouse, France, 1984

(19) Eichert D., S. H.; Combes, C.; Rey, C. Specific characteristics of wet nanocrystalline apatites. Consequences on biomaterials and bone tissue. *Key Eng. Mater.* **2004**, *254*, 927−930.

(20) Ironside, M. S.; Duer, M. J.; Reid, D. G; Byard, S. Bisphosphonate protonation states, conformations, and dynamics on bone mineral probed by solid-state NMR without isotope enrichment. *Eur. J. Pharm. Biopharm.* **2010**, *76* (1), 120−126.

(21) Yesinowski, J. P; Eckert, H. Hydrogen environments in calcium phosphates: proton MAS NMR at high spinning speeds. *J. Am. Chem. Soc.* **1987**, *109* (21), 6274−6282.

(22) Grossmann, G.; Grossmann, A.; Ohms, G.; Breuer, E.; Chen, R.; Golomb, G.; Cohen, H.; Hägele, G.; Classen, R. Solid-state NMR of bisphosphonates adsorbed on hydroxyapatite. *Magn. Reson. Chem.* **2000**, *38* (1), 11−16.

(23) Jäger, C.; Welzel, T.; Meyer Zaika, W.; Epple, M. A solid state NMR investigation of the structure of nanocrystalline hydroxyapatite. *Magn. Reson. Chem.* **2006**, *44* (6), 573−580.

(24) Wang, Y.; Azaïs, T.; Robin, M.; Vallée, A.; Catania, C.; Legriel, P.; Pehau-Arnaudet, G.; Babonneau, F.; Giraud-Guille, M. M; Nassif, N. The predominant role of collagen in the nucleation, growth, structure and orientation of bone apatite. *Nat. Mater.* **2012**, *11*, 724−733.

(25) Eichert, D.; Drouet, C.; Sfihi, H.; Rey, C.; Combes, C. Nanocrystalline apatite-based biomaterials: Synthesis, processing and characterization. *Biomater. Res. Adv.* **2008**, 93.

(26) Errassifi, F.; Menbaoui, A.; Autefage, H.; Benaziz, L.; Ouizat, S.; Santran, V.; Sarda, S.; Lebugle, A.; Combes, C.; Barroug, A.; Sfihi, H..; Rey, C. Adsorption on apatitic calcium phosphates: Applications to drug delivery. In *Advances in Bioceramics and Biotechnologies*; Narayan, R., McKittrick, J., Eds.; John Wiley & Sons, Inc.: Hoboken, NJ, 2010.

(27) Al-Kattan, A.; Errassifi, F.; Sautereau, A. M.; Sarda, S.; Dufour, P.; Barroug, A.; Dos Santos, I.; Combes, C.; Grossin, D.; Rey, C.; Drouet, C. Medical potentialities of biomimetic apatites through adsorption, ionic substitution, and mineral/organic associations: Three illustrative examples. *Adv. Eng. Mater.* **2010**, *12* (7), B224−B233.

(28) Gustavsson, J.; Ginebra, M.; Engel, E.; Planell, J. Ion reactivity of calcium-deficient hydroxyapatite in standard cell culture media. *Acta Biomater.* **2011**, *7* (12), 4242−4252.

(29) Bonnery, M.; Bouisset, M..Sole, R. Monohydrate of the disodium salt of 4-chlorophenylthiomethylene-bisphosphonic acid, its preparation and pharmaceutical compositions containing it. EP Patent 0,582,515, 1994.

(30) Cukrowski, I.; Popovic, L.; Barnard, W.; Paul, S. O.; van Rooyen, P. H; Liles, D. C. Modeling and spectroscopic studies of bisphosphonate-bone interactions. The Raman, NMR and crystallographic investigations of Ca-HEDP complexes. *Bone* **2007**, *41* (4), 668−678.

(31) Eichert, D.; Sfihi, H.; Combes, C.; Rey, C. Specific characteristics of wet nanocrystalline apatites. Consequences on biomaterials and bone tissue. *Key Eng. Mater.* **2004**, *254*, 927−930.
(32) Boanini, E.; Gazzano, M.; Rubini, K.; Bigi, A. Composite nanocrystals provide new insight on alendronate interaction with hydroxyapatite structure. *Adv. Mater.* **2007**, *19* (18), 2499−2502.